Research Internship Report - Infrared Laser-Locking and Michelson Wavemeter

LANORE Corentin

March - July 2021

ÉCOLE POLYTECHNIQUE
PROMOTION X2018

Option : Department of Physics
Field : PA "De l'atome au matériau"
Referent : Luca Perfetti
Tutor : Alexei Ourjoumtsev
Supervisor : Sébastien Garcia
Location : Quantum Photonics Team - Collège de France - Paris 75005 - FRANCE

Contents

1 Abstract

ENGLISH

The main subject of my internship has been to lock at a frequency of 1529 nm laser and to develop a wavemeter based on interference of two lasers in a Michelson interferometer. This wavemeter has the purpose to precisely tune the infrared laser which allowed us to lock it on a given wavelength. To put the wavemeter in a nutshell, a first laser will interfere with itself in a Michelson interferometer with a varying optical path and a second laser will also interfere in this very same interferometer with the same varying optical path. The difference in these two interferences signal allows us to compute the wavelength of the second laser, given with the wavelength of the first laser, with a precision : statistical relative precision of 1.30×10^{-6} and measurement trueness with a relative precision of 4.31×10^{-5}
.

The characterization of the wavemeter has given rise to questions about its effectiveness as it seems to rival commercial wavemeters because of its interesting characteristics : the short sweep length and its short sweeping time. Its effectiveness seems to steam from the way we use the data acquired which consists of a curve fitting, making better use of the data compared to what is usually done.

Through my internship I have acquired several technical skills such as electronics, manipulation of optical set-up, signal treatment, programming with SystemVerilog and Python and have consolidated several knowledge such as atomic physics, laser physics and general optic.

FRANCAIS

Le sujet principal de mon stage a été de mettre en place le vérouillage de fréquence d'un laser ayant pour longueur d'onde 1529 nm ainsi que le développement d'un lambdamètre basé sur les interférences entre deux lasers dans un interféromètre de Michelson. Ce lambdamètre a pour but de régler précisément le laser infrarouge afin de le vérouiller sur une transition atomique. Pour résumer succinctement le fonctionnement du lambdamètre, un premier laser interfère avec lui-même dans un interféromètre de Michelson, dont le chemin optique varie. Un second laser entre également dans cet interféromètre et interfère aussi avec lui-même avec les mêmes variations de chemin optique. La différence entre ces deux signaux d'interférences nous permet de calculer la longueur d'onde du second laser connaissant celle du premier avec une précision : précision relative statistique de 1.30×10^{-6} et une justesse de mesure avec précision relative de 4.31×10^{-5}

La caractérisation de l'ondemètre a soulevé des questions d'efficacité étant donné sa capacité à rivaliser avec des systèmes commerciaux, notamment avec sa faible longueur de balayage et son faible temps d'intégration. Son efficacité semble provenir de la manière dont les données sont traitées : on utilise un ajustement de courbe ce qui semble être une meilleure utilisation des données que ce qui est fait habituellement.

Durant mon stage, j'ai acquis des compétences techniques en électronique, en manipulation de montages optiques, en traitement du signal et en programmation en SystemVerilog et Python et j'ai consolidé mes connaissances théoriques en physique atomique, physique des lasers et en optique.

2 Introduction

The team "Quantum photonics' in which I have been integrated during my internship is part of the Physics Institute of Collège de France. The experiment on which they are working on is composed of an optical cavity in which is placed a cloud of rubidium atoms with few Rydberg-level excitation. One of the main objectives is to use the strong interaction between Rydberg's atoms in the cold cloud in order to induce strong interaction between photons inside the cavity. The current focus of the team is to use these strong interactions to produce non-classical quantum states of light outside the cavity thanks to manipulation of Rydberg excitation; Many phenomena have already been observed such as Rabi oscillations of a single collective Rydberg excitation and there is hope to observe "cat states" of light soon enough.

For the strong interaction between photons inside the cavity, one way to do such a thing has been described in [1] which use the modulation of an intermediate atomic level. The upcoming objective is to reproduce partially the experiment of the article in order to get new results out of it.

We want to lock an InfraRed laser in order to do Floquet engineering, which have for purpose to alter the spectrum of rubidium and make it compatible with the spectrum of a cavity which give rise to interacting polaritons. The general idea to reach this goal is to frequency modulate the IR laser locked on an intermediate atomic level, matching the energy spacing between the modes of the cavity. With Rydberg's dressing of the cold atoms, theses polaritons interact strongly and thus provide interesting prospects in quantum information.

In order to do so, my internship's goal has been to set up a wavemeter to measure the laser frequency and the locking of the laser at this rubidium's atomic transition. In order to present it, we will firstly describe the optical set-up, in a second part discuss the algorithm of the wavemeter and it's integration, then we will discuss the locking of the infrared laser and lastly we will conclude. A non negligible part of my internship won't be discussed here, involving confidentiality and intellectual property.

3 Optical Set-up

3.1 Overview

We will firstly describe the optical set-up without all the technical details in order to simplify the concept of the whole set-up. In order to do so, we will divide the system in three different components : The "NIR-locking", the "Interferometer" and the "IR-locking" as shown in Figure 2.

The first component is the "NIR-locking" which has for purpose to lock the NIR (Near InfraRed, wavelenght of 780 nm) laser to a given wavelength. Its mode of operation will be explained in the "Laser Locking" subsection that follow. It is this laser that will act as the reference for the measurement of the second laser, the IR one as it will be explained in subsequent sections. As we will see it, the lock of this laser use the technique of "saturation absorption" which will be broadly explained.

The second component is the "Interferometer" in which there are the two laser inputs and the acquired signal output. There are no peculiar think as it's just a regular Michelson interferometer. Its implementation will be thoroughly explained in the "Wave-meter set-up" subsection and the algorithm used to compute the wavelength our of the data acquired. Optimization considerations can be found in the annex "Fourier Transform vs Curve fitting".

The third component is the 'IR-locking", which will provide a precision out of the interferometer : if we know both laser's wavelength with a given precision (because of the locking on a spectral line of rubidium for example), we can then measure with the spectrometer the wavelength and give its precision. The locking of this laser is tightly linked with the locking of the NIR laser as it will also allow us to lock the IR laser before characterizing it.

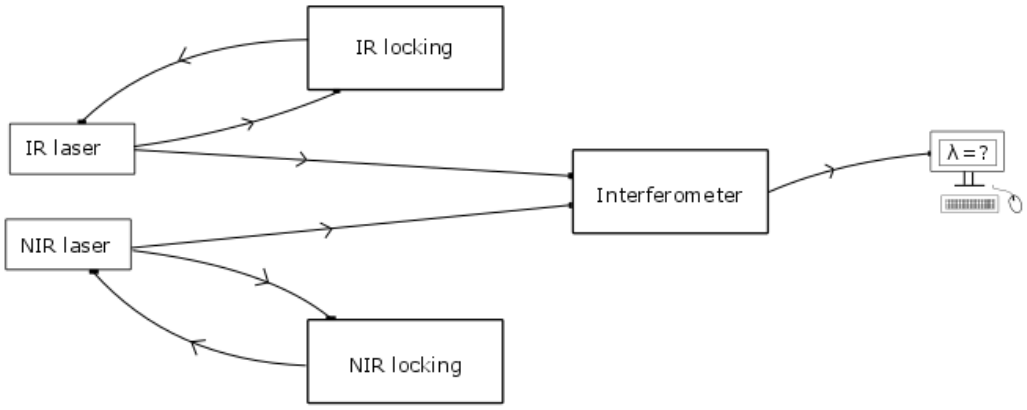

Figure 2: Simplified schematic of the experiment

3.2 Laser Locking

In this section we will describe why we are required to lock our lasers, how can one lock a laser and how it is integrated in the set-up.

With rubidium, there is only one electron on the last unfilled band which make it a useful atom when we are trying to understand the atomic transitions. In the Figure 3 has been drawn several energy level of rubidium relevant for our purpose.

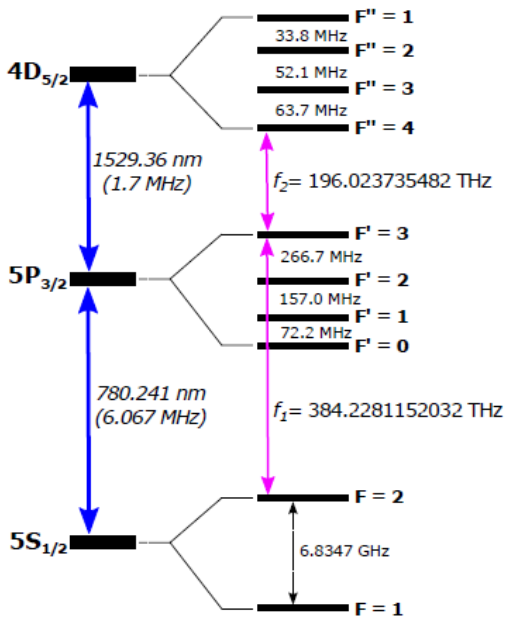

Figure 3: Some spectral lines of rubidium 87 from [2]. Numbers in brackets are full-width-half-maximum linewidths.

Firstly, we want to lock the NIR (Near InfraRed) laser as it will be the reference for computing the wavelength of the IR laser. Secondly we want to lock the IR (InfraRed) laser because it will be used for the main experiment (it is required to be locked on the right frequency) and moreover we can characterize the wavemeter : we can just measure the IR wavelength with the interferometer and we obtain its precision (assuming it doesn't depend drastically of the actual wavelength). Finally we have both lasers locked and a characterized wavemeter.

Now in order to lock a laser we use a cell containing atoms in the form of vapor, which will absorb the light in given spectral band ; we can suggest that we can simply analyse the absorption spectra and adapt the different parameters of the laser that can influence the output wavelength (the current, the temperature).

Let's take a look at the NIR locking component in Figure 4:

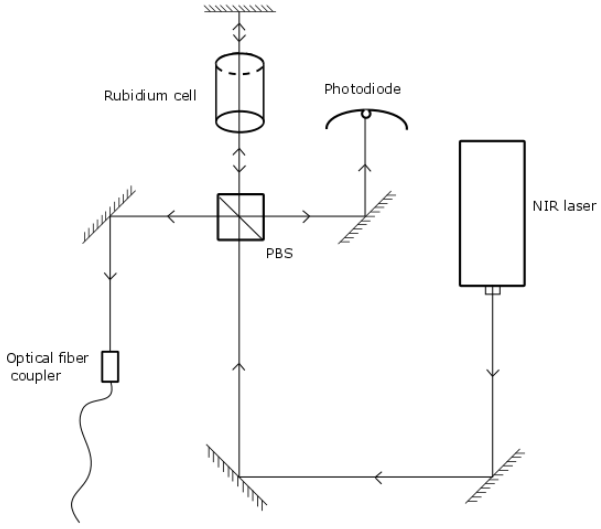

Figure 4: Schematic of the NIR locking

The NIR beam is split in two beams on the PBS, the first one is directly sent to the interferometer through an optical fiber and the second one passes through a rubidium cell two times and then is analysed with a photodiode. We can see in Figure 5 the signal acquired on the photodiode (the NIR laser is in scan mode, scanning a given wavelength band). Here we make use of the "Saturated Absorption" which will be explained (as we can see in the schematic, the laser pass through the rubidium cell two times).

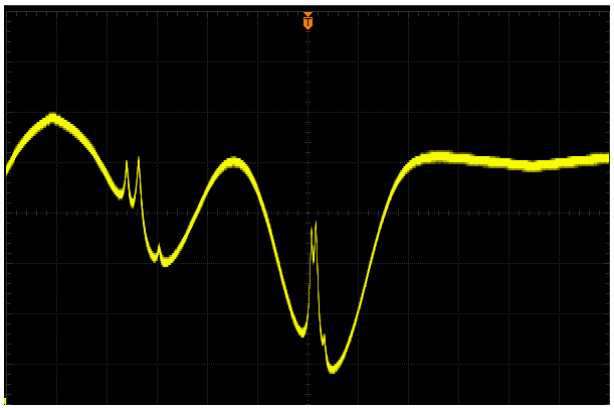

Figure 5: Transmission curve of the scanning NIR laser

The first thing we observe on that figure are the two broad dips in the transmission curve which are a feature of the reduced transmission through the rubidium cell. In order to give quantitative analysis, we can derive the known formula of the Doppler broadening [3] :

$$\Delta f_{FWHM} = \sqrt{\frac{8k_{\mathrm{B}}Tln(2)}{mc^2}} f_0$$

Which is the Full Width at Half Maximum of broadened frequency f_0 at a given temperature of

the vapor of rubidium which give the Boltzmann distribution of velocities of a perfect gas and allow the computation of this relation. k_B is the Boltzmann constant. With our current values, we get $\Delta f_{FWHM} = 0.5$ GHz.

The Doppler effect widening the transition width is quite easy to grasp as it steams from the different velocities of the atoms in the cell that observe different wavelengths in their own referential : $f = f_0(1 + \frac{v}{c})$ with v the velocity of the atom.

Furthermore we observe on these broad dips several spikes which are characteristics of absorption reduction. In order to understand why such absorption reduction appear here, we have to explain how "Saturated absorption" actually works [4],[5],[6],[7]. In our rubidium cell, there are two lasers (which are actually the same but passing two times through the cell in our case) the first one is the "pump beam" with a relatively high intensity, which will almost totally saturate a transition if at the adequate wavelength (the atoms are in a superposition in both the "exited" and the "ground" state) and the counter propagating beam, the "probe beam", will pass through the rubidium cell and is then analysed on a photodiode.

The key here to understand the process here is to think with one wavelength at a time (even if the laser is actually scanning over time several wavelength, at a given time the laser has one define wavelength). If we restrain ourselves with only one atomic transition, we can quite easily understand that only the atoms with a null velocity will both interact with the pump and the probe beam : otherwise they won't observe the same wavelength from the pump and the probe in their own referential.

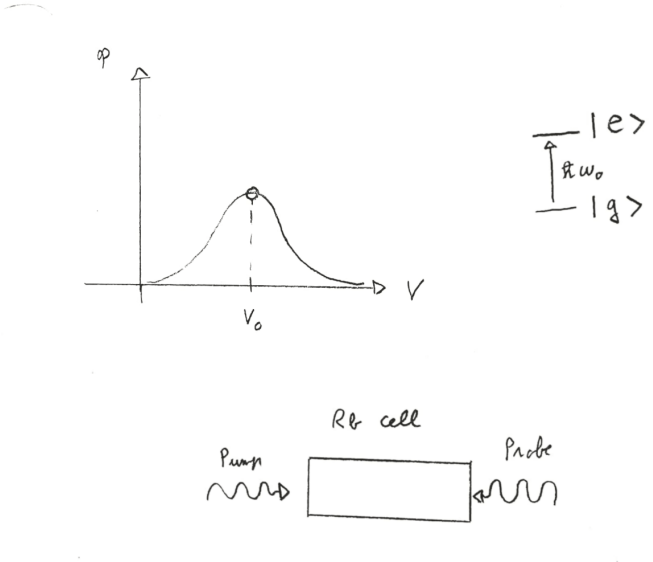

Figure 6: The top left panel represents the Boltzmann distributions of velocities with v_0=0, the top right panel shows the energy-level structure of a two-level atom. The lower panel pictures the experimental configuration of counter propagating lasers in the gas cell.

So if the atoms have not a null velocity and knowing that the pump beam consists of the first passage of the laser and the probe beam consists of the second passage of the beam, then at both the beam will be partially absorbed (because of the Doppler Broadening effect) because they do not

address the same "class" of atoms.

Here we can define a relation operation on atoms : If we restrict ourselves to the real axis for the velocities, A is the set containing our atoms which each have a velocity on this axis (here it's the laser's axis), then :

$$a_1, a_2 \in A \tag{1}$$

$$a_1 \sim a_2 \Leftrightarrow v_1 = v_2 \tag{2}$$

We can then take the quotient of A by $\sim$, and we get $A/\sim$ which contain the classes of atoms with a given velocity. For example the class of one atom with a null velocity contain all the atoms with a null velocity. So when we said that the pump and the probe beam do not address the same class of atoms, we had in mind that the atoms observe a different apparent wavelength from them.

If the atoms have a null velocity then the pump and the beam address the same class of atoms and thus if the pump saturate the transition then the probe (the second passage of the laser) is not absorbed as much and gives rise to a transmission peaks, which finally explain some of the spikes in the Doppler effect broadening.

However, atoms have actually several transitions which can be quite close in frequency : let's consider an atom with two transitions (close enough to the laser's wavelength).

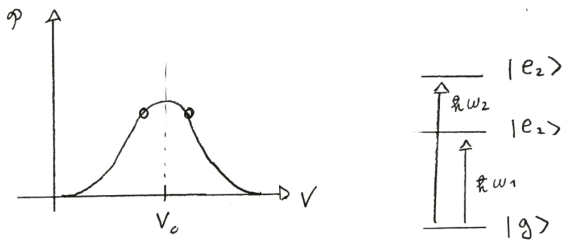

Figure 7: The left panel represents the Boltzmann distributions of velocities with v_0=0, the right panel shows the energy-level structure of a three-level atom.

If the atoms have a null velocity, then they observe the same wavelength from both the pump and the probe beam and thus we are back in the first case of a single atomic transition as the laser will interact with one of the two atomic transitions.

However if the atoms do not have a null velocity, then for a given wavelength, a given velocity-class of atoms will be resonant with the pump beam for a given transition and also resonant with the probe beam for the other transition. In order to understand this, let's assume our pulsation of the laser ω fixed and that atoms of a class +v (we give a direction to our axis, the probe comes from the positives) are transition-1 resonant for the probe beam.

$$f_1 = f_{laser}(1 + \frac{v}{c})$$

With f_{laser} the actual laser's frequency, f_1 the frequency observed of the probe by the atom. Moreover let's suppose that this same class of atoms are transition-2 resonant for the pump beam.

$$f_2 = f_{laser}(1 - \frac{v}{c})$$

With f_2 the frequency observed by the atom of the pump laser. If the pump beam is strong enough, it will saturate the transition-2 and thus the transition-1 will be almost transparent even if the probe beam is in resonance. This very same analysis can be done with atoms of the class -v with the exact same wavelength as they will be transition-2 resonant with the pump and transition-1 resonant with the pump. This gives rise to a spike of transmission known as "crossover".

The transitions on which the NIR laser will be locked is the crossover between $(5S_{1/2}, F = 2 \longrightarrow 5P_{3/2}, F^{'} = 1)$ and $(5S_{1/2}, F = 2 \longrightarrow 5P_{3/2}, F^{'} = 3)$. Let's compute the absolute wavelength of the laser at this crossover.

$$f_1 = (1 - \frac{v}{c})f_{laser} \tag{3}$$

$$f_2 = (1 + \frac{v}{c})f_{laser} \tag{4}$$

So we can rewrite

$$f_1 - f_2 = 2\frac{v}{c}f_{laser} \tag{5}$$

$$f_1 + f_2 = 2f_{laser} \tag{6}$$

So we can extract f_{laser} and v the velocity of the atoms which are addressed by the laser because f_{at_1} and f_{at_2} are precisely known [4].

$$\lambda_{laser} = 780.241251\text{nm} \tag{7}$$

$$v = 165.2\text{m/s} \tag{8}$$

We will now explain the process used to lock a laser [8], [9]. The first observation is that the absorption curve gives us locally even function centered on the atomic transitions, which is not adapted if we want to lock it with an algorithm : if the error signal corresponds to the difference of absorption with a reference one, how can we know if our wavelength is too low or too high when both cases give the same response because of the parity of the function ?

The idea is to extract the derivative of the absorption curve which will transform the even curve into an odd one centered on the transition, breaking the apparent symmetry and thus allowing a feedback loop to lock the laser.

In order to get the derivative of the absorption curve, we use a method known as frequency modulation spectroscopy [10]. The general idea is to modulate the laser's current of frequency ω with a given frequency modulation Ω which in the case of weak modulation amplitude will give rise to "side bands" on the laser frequency $\omega + \Omega$ and $\omega - \Omega$.

This phase modulation will give rise to "beats" on the photodiode of the probe beam, when multiplying this signal with the modulating signal and applying a low-pass band filter, we can extract the derivative of the absorption curve.

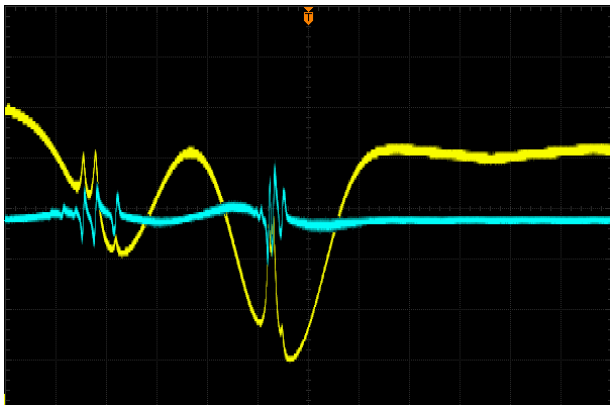

Figure 8: Absorption curve (yellow) and its derivative (blue) on the scanning NIR laser

Given this derivative of the absorption curve, we can then reduce the spectral range of the NIR laser's scanner.

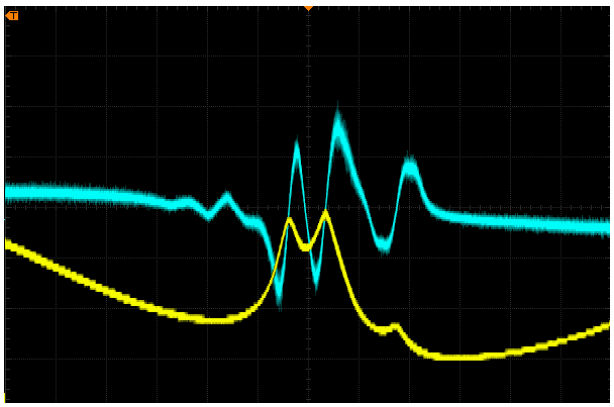

Figure 9: Zoom on Absorption curve (yellow) and its derivative (blue) on the scanning NIR laser

Here we can easily understand why the imparity of the derivative curve is so useful.
In order to actively lock the laser, we employ a feedback loop based on the "PID controller". PID stands for Proportional, Integral and Derivative. Let's give ourselves an error signal :

$$\begin{aligned} \epsilon : \mathbb{R} &\to \mathbb{R} \\ t &\mapsto \epsilon(t) \end{aligned}$$

We have a parameter X on which we can interact on in order to change the error signal (which will likely change over time even without changing the parameter). The goal of our algorithm is to stay the closest possible to the value $\epsilon_0 = 0$ interacting only through the parameter X. If we take for example a laser's wavelength our error signal is it's actual wavelength minus the desired one and the parameter is the current applied on the laser.

For example, let's respond to the error signal as such : $X(t) = A\epsilon(t)$ with A a constant : if you are at the right wavelength and if we confine ourselves to an easy modeling of the system, then there won't

have any problems. But with the slightest variation of wavelength, we would have to correct it by, let's say, increasing the current. However, given the time the system will respond to such new current, it will be probably already too high and would have to reduce it and so on and so forth. This is the "Proportional" part of the PID which can in some case be sufficient if the reactivity of the system to the parameter is sufficient.

But in the case of our laser it might not seem quite enough and it seems likely that it will start oscillating around the desired wavelength without ever reaching it : we have an oscillator. With such analogy, we can then describe our system as such and try to find ways to stabilize it. One way is usually to add a damper and to tune it in order to reach the non periodical critical regime. The damping on an oscillator usually comes from a derivative of the position term, we can then take $X(t) = A\epsilon(t) + \tau\frac{d\epsilon}{dt}$ with τ a characteristic time. This is the "Derivative" term.

We lastly one of the most important part is the "Integration" term in order to correct a possible offset of the final value over time. Because a proportional control G reduce the error signal by a factor of $\frac{1}{1+G}$ but doesn't make it null.

For the locking of our NIR laser, we use a commercial analog system sold by Topica, the manufacturer of the laser.

3.3 Wave-meter set-up

In this section, we will go further into details considering the physical set-up of the interferometer.

It is the main component of the setup, it consists of two laser entry, a linear piezoelectric positioning system (P-611.1 from PI), silver and dichroïc mirrors and photodiodes. The two rays enter the interferometer and each inteferes with itself on the beam splitter.

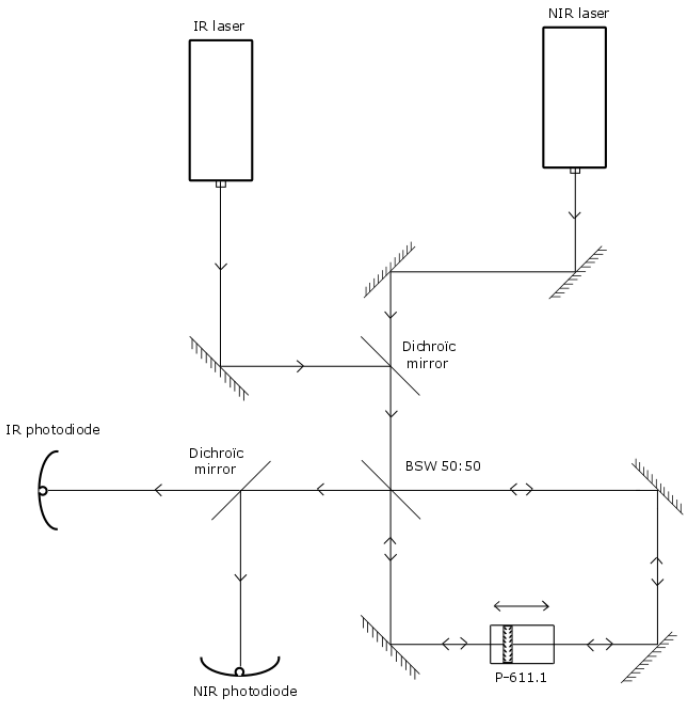

Figure 10: Schematics of the the interferometer

Now we can simply vary the optical path with the piezoelectric translation (applying the right electric signal on it) and observe the variation of interference. The bottom-right part of the schematic is the actual interferometer, in which the pizeoelectric translation will be motioned over time in order to acquire data, each sweep will be "one measurement".

4 Wavemeter operation

4.1 Material Integration

In order to acquire data, we have to use different devices which have physical limitations. Firstly, we used a PXI chassis (from National Instruments) which contains acquisition cards that transform analog signal into numeric signal given a rate (the acquisition rate of the card) and store these data which are later on analyzed with a python code on a computer. There also are output cards that allow to transform numerical signals into analogical one.

The acquisition card we use has a rate of 250.000 points per seconds and a question arise : "What is the best sweeping time of the translation stage in order to get a sufficiently precise data acquisition ?" Knowing that we mainly will have a cosine-like function out of the interference pattern, we can for example say that we need at least 4 points for each periods of the cosine. Another possibility is to totally invert the problem and ask for a sufficiently low statistical dispersion associated with the measurement. As it will be shown, 50ms seem to be the most adapted to the limits of translation of the piezoelectric.

There is a question that is still unanswered yet, what kind of signal should we put into the piezoelectric translation stage ? We could for example use a triangular shaped signal, but the total acceleration might be a bit too harsh, so we have preferred to use a smooth function for the signal. More precisely as shown in Figure 11 we use an "S" curve that minimize the jerk and the vibration's energies.

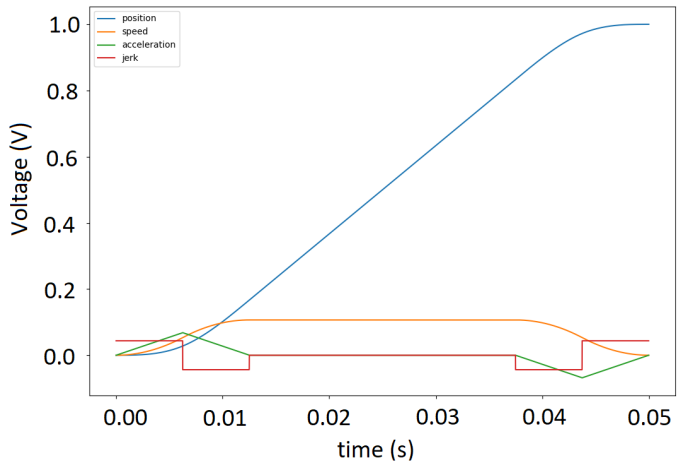

Figure 11: Signal applied on the Piezoelectric translation for one measurement in blue, the associated speed in orange, acceleration in green and jerk in red

With this "S" curve signal and in the middle of the signal, we get these data when sweeping the deck with given time :
-50 ms scan : 12.500 points, approximately 18 points per period,
-25 ms scan : 6250 points, approximately 7 points per period,
-12.5 ms scan : 3125 points, approximately 3 points per period.

One interesting point is that asking for a sufficiently low statistical dispersion in the measurement of the wavelength gives us the lower limit of the number of points per period. We can give for example the standard deviation (of 1600 measurements) for the given sweep time :

-50ms scan : approximately 0.0021 nm, -25ms scan : approximately 0.0052 nm

As we can see, the statistical dispersion is multiplied by 2 and the statistical error on the mean would be reduced by a factor ln(2), so it justifies the use of the 50ms scan.

4.2 Extracting the unknown wavelength form the signals

In this part, we will precisely explain how given the interferences of both lasers in the interferometer enables us to compute the wavelength of one of the laser given the other. The point is that the optical path has the same variation with respect to time for both lasers.

The variation of optical path is given by a "scan", which consists of a sweep of the piezoelectric translation over a length of $L = 120\mu m$. Each scan permits the computation of λ_{IR} and thus defines a "measurement" of the wavelength. One measurement (scan) has a duration of 50 ms and acquires 12.500 points.

Let's observe on Figure 12 what we obtain after a scan of the translation after normalization between 0 and 1.

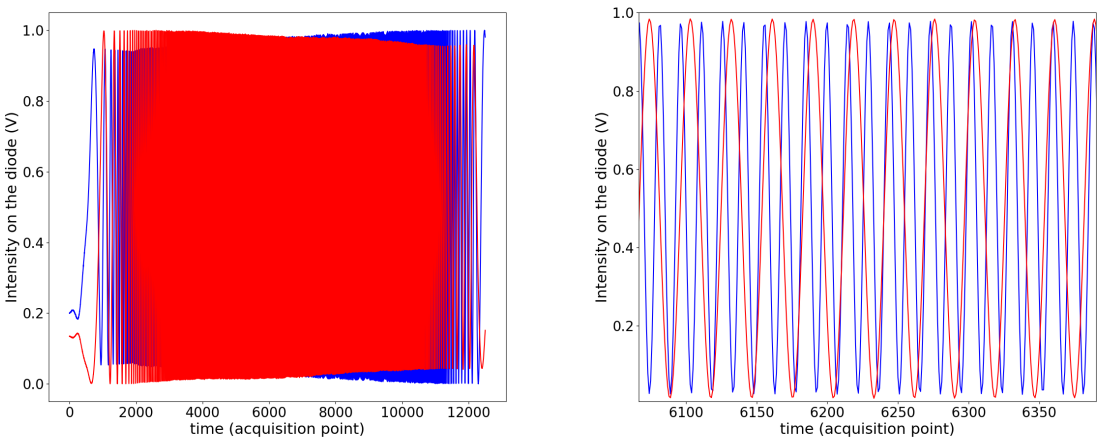

(a) Re-normalized signals

(b) Zoom on the Re-normalized signals

Figure 12: Interference signal acquired on a 50ms scan of the piezoelectric deck

If we only consider one of the normalized curve (either the blue or the red one), we can then extract the phase applying an arrcos to $2I - 1$ (being of the form cos(x)).we see that, up to an offset and a scaling factor of 2, it is the cosine of a time-varying phase. To extract this phase, we first apply an arccos to the signal. In order to get only an increasing function, we multiply this arrcos(cos(x)) with the sign of the derivative of cos(x), we obtain the curves given on the next figure.

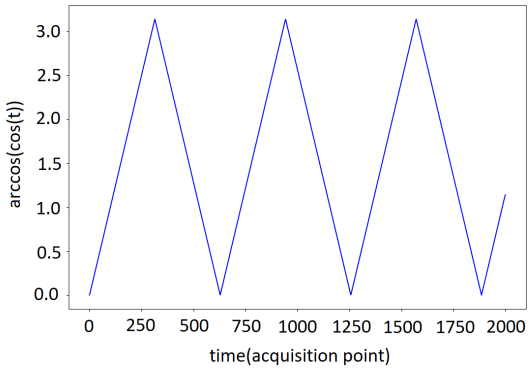

(a) Plot of arccos(cos(x))

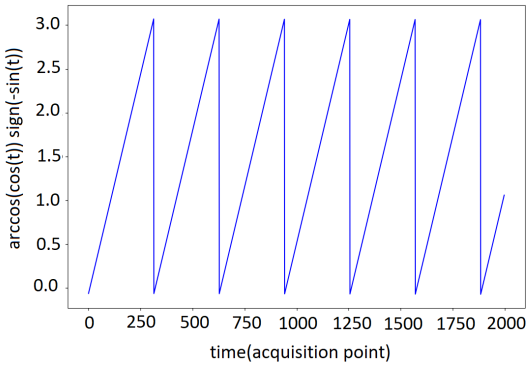

(b) Plot of arrcos(cos(x))sign($\frac{dcos(x)}{dx}$)

Figure 13: Plots of operation applied on a cosinus function

Now we can apply a python function "unwrap" which reconstructs the phase out of this function (at each discontinuity higher than π, we add 2π), with our example cos(x), we simply get a linear function, which is the phase of our function. If we had a cos(f(x)), we would simply get f(x). This whole process has for purpose to extract the phase without the 2π restriction, if we apply this to our signals we obtain the function of the translation position with different prefactor. After applying this "unwrap of the phase" process on both obtained signals, we get two "phases" which will be denoted ϕ_{IR} and ϕ_{NIR}.

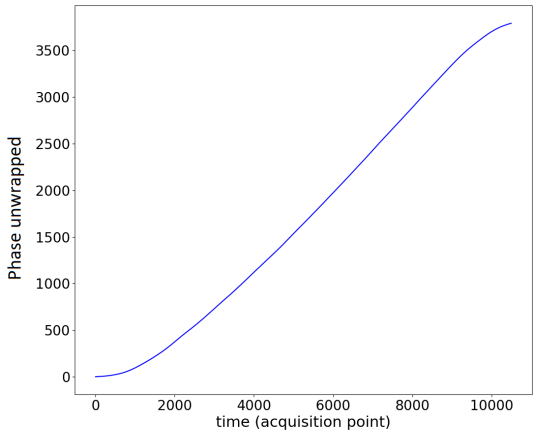

(a) Unzoomed curve

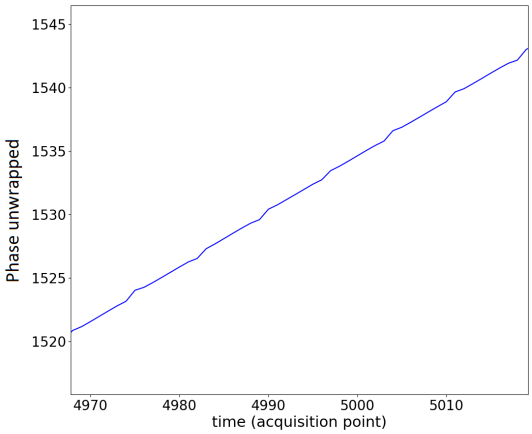

(b) Zoomed curve

Figure 14: Plots of the unwrapped phase with one of the the signals

We can observe on the zoomed signal that it is not perfectly smooth. The origin of this has been retraced during my internship to the varying contrast of interference observed on the signal (we can see it quite clearly on the first figure).

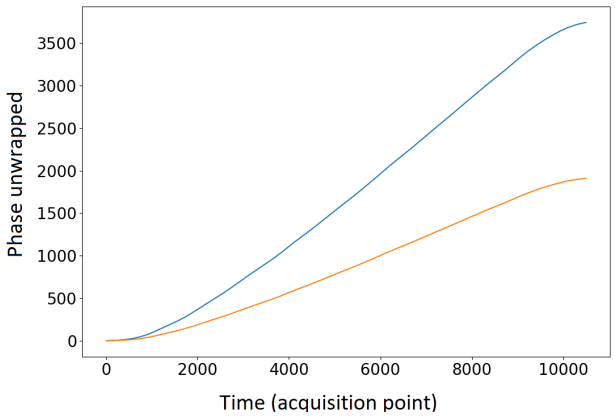

Figure 15: ϕ_{IR} and ϕ_{IR} as a function of time

We have, with $\delta(t)$ the position of translation :

$\phi_{IR} = k_{IR}\delta(t) + \phi_{0,IR}$ and $\phi_{NIR} = k_{NIR}\delta(t) + \phi_{0,NIR}$

And so that means that $\phi_{NIR} = \frac{k_{IR}}{k_{NIR}}\phi_{IR} + C$
where C is a constant depending on the initial phase offsets $\phi_{0,IR}$ and $\phi_{0,NIR}$, and on the wavevectors k_{IR} and k_{NIR}.

In other words, there is a linear relation between ϕ_{IR} and ϕ_{NIR}, which mean that if we plot $\phi_{IR}(\phi_{NIR})$ we should get a linear curve with a linear coefficient given by $\frac{k_{IR}}{k_{NIR}}$. Knowing one out of these two wave vectors, we guess the other. The last thing to do is then to plot this $\phi_{IR}(\phi_{NIR})$ and fit a linear curve.

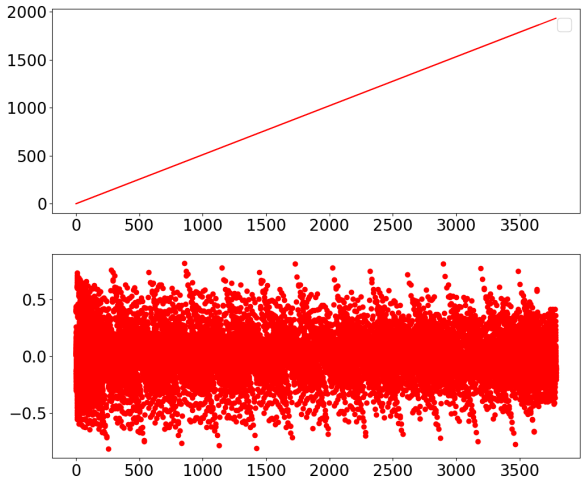

Figure 16: $\phi_{IR}(\phi_{NIR})$ and the "residuals" of the linear fit

In this process, we have to take into account an important thing : The whole experiment is done in the air, not in vacuum. In order to take that into account, we have to use a conversion of the different wavelength : Eldén formula has been integrated into the code from this website :"https://emtoolbox.nist.gov/Wavelength/Documentation.asp".

We use this approximation to get the IR wavelength $\lambda_{IR} = \frac{1}{alpha} \frac{\lambda_{NIR} n(\lambda_{NIR}, \boldsymbol{\mu})}{n(\lambda_{IR}, \boldsymbol{\mu})}$

The algorithm depicted above has firstly been tested with simulated signals (to which we added noises to verify its robustness) and seemed sufficiently robust to allow the relative precision that we sought (10^{-6}). Moreover as it is explained in the annex "Fourier Transform" section 7.1, the way the algorithm treats the data (fitting a curve) seems much more efficient than just counting the number of local extrema and the initial and final phases [11].

4.3 Precision of the measurement

In this section, we will discuss the statistical precision of the wavemeter. In order to do so, we lock the NIR laser and measure the dispersion of the different wavelengths.

We lock the NIR laser (at 780.246452 nm in vacuum, with a Rb cell) and proceed to take 3200 measurements set (which are divided in 32 subsets). The mean and standard deviation are from statistical process and not a fitting of a Gaussian curve for example.

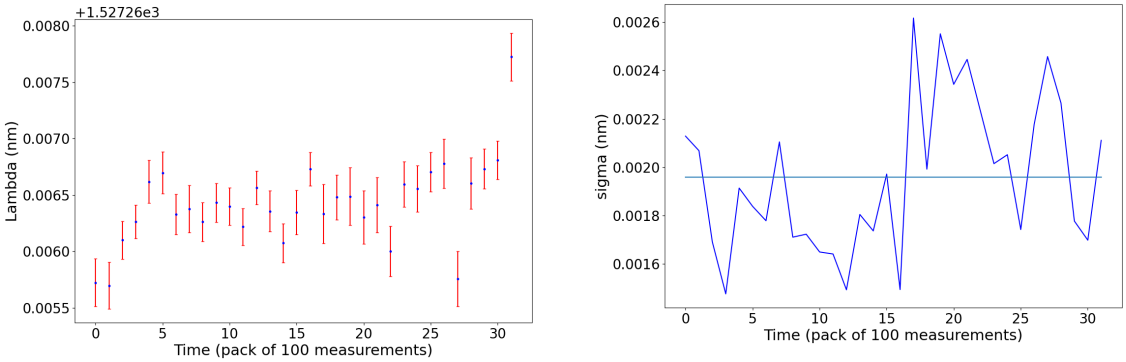

(a) Mean value with SE_M (standard error) as error bars

(b) Statistical dispersion of the mean and their mean value

Figure 17: Plots of a 3200 measurement set divided in 32 subsets

As we can see in Figure 17, there are significant variations over time of the mean which impair the precision on a long time period of measurement. We have to lock the IR laser in order to reduce this. The mean standard deviation on 32 different subset (100 measurement each) is 0.0020 nm, so the relative precision of a single measurement is 0.0020/1527=1.30×10^{-6} . We can also fit a Gaussian curve on an histogram of a 3200 measurement set with the NIR laser locked :

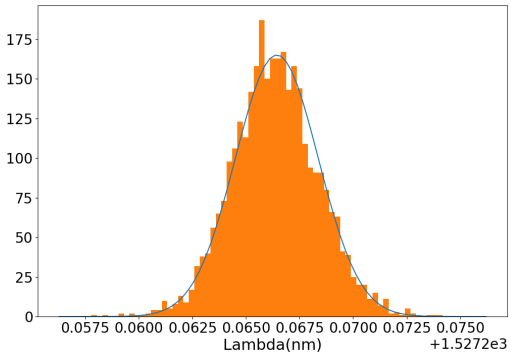

Figure 18: Histogramm λ_{IR} (nm) fitted with a Gaussian curve

$\lambda_{IR} = 1527.03112$nm, Standard deviation= 1.49×10^{-3}nm

We can then deduce that the statistical error is quite low; For example in [12] they obtain experimentally a for a 20s measurement $\frac{\Delta\lambda}{\lambda} = 2 \times 10^{-8}$ and about the same for [11]. As for commercial wavemeter, we can take for example this one from ThorLabs : `https://www.thorlabs.com/newgrouppage9.cfm?objectgroup_id=5276`, which have a relative resolution of 2×10^{-7}. The point here is that our apparatus has a relative resolution which is quite interesting given the low acquisition time for one measurement (50ms) and the very short translation (120 μm) which compete with commercial devices.

The second point which will be discussed is the measurement trueness of the apparatus.

Once the IR laser is locked on a given wavelength which is precisely known [2], knowing the statistical precision of the wavemeter we can compare the value we measure with a precisely known one.

For an alignment done with the eyes on a length of approximately one meter, we measured the wavelength obtained when both lasers are locked. We took 1600 measurement. The locking of the NIR laser is on the crossover between $(5S_{1/2}, F = 2 \longrightarrow 5P_{3/2}, F^{'} = 1)$ and $(5S_{1/2}, F = 2 \longrightarrow 5P_{3/2}, F^{'} = 3)$ and the IR laser is locked on the $(5P_{3/2}, F' = 3 \longrightarrow 4D_{5/2}, F^{"} = 4)$.

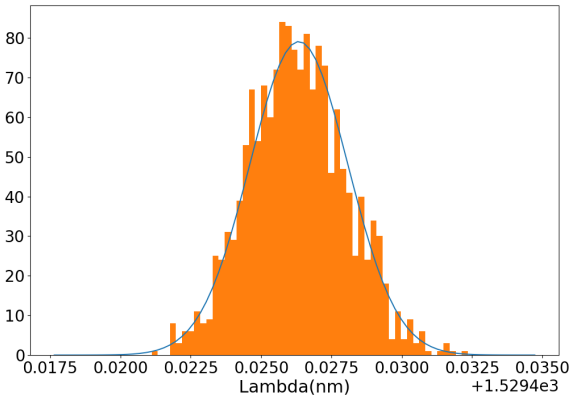

Figure 19: Histogram of wavelength obtained on a 1600 measurement set with both laser locked with a Gaussian fit

$\lambda_{IR} = 1529.426nm$, Standard deviation= $0.0017nm$

We can then compute the relative error of the measurement with respect to the wavelength in [2] of the IR laser. Out of this we get $\frac{\delta\lambda_{IR}}{\lambda_{IR}} = -4.31 \times 10^{-5}$. We can then compare with the uncertainties that have been computed in the Uncertainty subsection below , and determine to what extent the measurement trueness can be improved.

4.4 Uncertainty

In this section we derive the uncertainty of the complete measurement process (the physical measurement and the algorithm).

Let's model the laboratory variables (such as the temperature, the pressure, the humidity, etc...) as uncorrelated random variables $(X_i)_{i\in I}$ with normal distribution and the "physical measurement" with instruments as a random variable M which is uncorrelated with the $(X_i)_I$. We note $J = I \cup \{i_M\}$ with $X_{i_M} = M$. We note here that the real laboratory variables have the mean values $\boldsymbol{\mu} = (\mathbb{E}[X_i])_{i\in J}$, the $(X_i)_I$ are the variables we use in the algorithm with a measurement uncertainty.

Here we use this random variable M in order to model the variations from the measuring instruments; Assuming the $(X_i)_I$ are constant random variables (with a null variance), the variance will comes from the measuring instruments. We do not explicit what this random variable exactly is, it

can be a vector containing all the acquired points of the diode voltage for example.

The method we use here is called the "sandwich method" [13] which assert that given a random variable Y defined as a function of random variables $f(X) = Y$, knowing $\boldsymbol{\mu} = (\mathbb{E}[X_i])_{i\in J}$ and $\boldsymbol{C} = (Cov(X_i, X_j))_{i,j\in J}$ with J the union of I and M we have approximately.

$$\mathbb{E}[Y] = f(\boldsymbol{\mu}) \text{ and } Var(Y) = (\nabla_{\boldsymbol{\mu}} f)^t \boldsymbol{C} (\nabla_{\boldsymbol{\mu}} f).$$

The point here is that there are no correlation between M and X_i, $\forall i \in I$. Firstable, let's suppose we acquire a pure signal (so the associated random variable M has a null variance) and derive the variance of Y coming from the laboratory parameters. Because the $(X_i)_I$ are uncorrelated one another, we can compute the uncertainties by fixing one parameter and fixing the others (by setting their variance to 0). With a pure signal, the algorithm gives us the parameter $\alpha = \frac{\lambda_{NIR,air}}{\lambda_{IR,air}}$ which is function of the real laboratory variables, we will now derive the uncertainties from each parameters. Let's define $n(\lambda, \boldsymbol{\mu})$ the optical index as a function of the wavelength and the parameters and λ_{NIR} λ_{IR} as the NIR and IR wavelength is vacuum.

If we consider the variance of Y coming from the random variable M, with the variance of the $(X_i)_{i\in I}$ null because of the null co-variance, then it is exactly the one that have been obtained while testing the algorithm with noise generated signals. (relative precision of 10^{-6}).

Let's introduce the different parameter that will influence the measurement :

-the temperature that change the optical index of air,
-the pressure that change the optical index of air,
-the humidity that change the optical index of air,
-the Gouy phase that change the effective wavelength of a Gaussian beam compared to a plane wave,
-the alignment between the IR and NIR ray that change the effective wavelength of one of the two beams.

We then have $\alpha(\boldsymbol{\mu}) = \frac{\lambda_{NIR}(\mu)}{\lambda_{IR}(\mu)} \frac{n(\lambda_{IR}(\mu),\boldsymbol{\mu})}{n(\lambda_{NIR}(\mu),\boldsymbol{\mu})}$ which have no uncertainty with a pure signal.

From this point, the algorithm can be reduced as $\lambda^m_{IR}((X_i)_I) = f((X_i)_I) = n(\frac{\lambda_{NIR}}{\alpha(\boldsymbol{\mu})}, (X_i)_I) \frac{\lambda_{NIR} n(\lambda_{NIR},(X_i)_I)}{\alpha(\boldsymbol{\mu})}$

The measured laboratory variables $(X_i)_I$ have a given uncertainty, we now denote one of these as U and fix the others.

What we compute in the algorithm is $\lambda^m_{IR}(U) = f(U) = n(\frac{\lambda_{NIR}}{\alpha(\boldsymbol{\mu})}, U) \frac{\lambda_{NIR} n(\lambda_{NIR},U)}{\alpha(\boldsymbol{\mu})}$, we then can just derive this expression with respect to U and divide it by λ_{IR} in order to get the relative error.

$\frac{\partial f}{\partial U}(\boldsymbol{\mu}) = \frac{\partial n}{\partial U}(\frac{\lambda_{NIR}}{\alpha(\boldsymbol{\mu})}, \boldsymbol{\mu}) \frac{\lambda_{NIR}}{\alpha(\boldsymbol{\mu})} n(\lambda_{NIR}, \boldsymbol{\mu}) + n(\frac{\lambda_{NIR}}{\alpha(\boldsymbol{\mu})}, \boldsymbol{\mu}) \frac{\lambda_{NIR}}{\alpha(\boldsymbol{\mu})} \frac{\partial n}{\partial U}(\lambda_{NIR}, \boldsymbol{\mu})$
We can then compute the variance of Y given the variances of the parameters:

$\frac{\delta \lambda^m_{IR}}{\lambda_{IR}} = -9.5308 \times 10^{-7}$ for an uncertainty in temperature of $\delta T = 1K$
$\frac{\delta \lambda^m_{IR}}{\lambda_{IR}} = 2.65 \times 10^{-9}$ for an uncertainty in pressure of $\delta P = 1kPA$
$\frac{\delta \lambda^m_{IR}}{\lambda_{IR}} = 1.92 \times 10^{-8}$ for an uncertainty in relative humidity of $\delta RH = 1\%$

We can also apply the formula of f in order to compute the uncertainty coming from the Eldén

formula : The uncertainty on n is : $\delta n = 3.2 \times 10^{-8}$, so we have an uncertainty of $\frac{\delta \lambda_{IR}^m}{\lambda_{IR}} = 6 \times 10^{-8}$.

The Gouy phase is a phenomena that arise when dealing with a Gaussian beam. If the beam is propagating toward the z axis, given cylinder framework with respect of this axis, if we restrict ourself to this z axis (r=0), we can write the electric field as a function of z :

$$E(z) = E_0 e^{-ikz+\gamma(z)} \text{ , with } \gamma(z) = arctan(\frac{z}{z_0}) \text{ and } z_0 = \frac{\pi \omega_0^2}{\lambda}$$

ω_0 is the waist of the beam and this $\gamma(z)$ is what we call the Gouy phase, it can have an influence on the apparent wavelength which we define as : $k_{app} = \frac{\partial E}{\partial z}$. This definition is quite intuitive as if we ignore the Gouy phase, $k_{app} = k$ and directly arise from the wave equation. So we have :

$$k_{app} = k + \frac{1}{z_0} \frac{1}{1 + (\frac{z}{z_0})^2}$$

The worst case scenario is when z=0, we then have $k_{app} = k + \frac{1}{z_0}$, which mean $\delta\lambda = \lambda_{app} - \lambda = 2\pi(\frac{1}{k+\frac{1}{z_0}} - \frac{1}{k})$, so finally we have $\frac{\delta\lambda}{\lambda_{NIR}} = -1.2163 \times 10^{-7}$ with $\lambda_{NIR} = 1529nm$.

After the locking of the IR laser, we struggled to understand why we had an error of 10^{-5} with measured wavelength in [2] for example : the variances obtained here did not account for it, we made a study in order to understand where this error was from.

We had our interferometer giving us statistically accurate measurement (we had a sufficiently low dispersion of measurement), the first step was to try to align again the two rays, firstly with the eye and secondly coupling both lasers in a same optical fiber at the output of the interferometer, but it was not enough, so we mapped the variation of wavelength with respect to the angle between the two rays, as shown in the next figure.

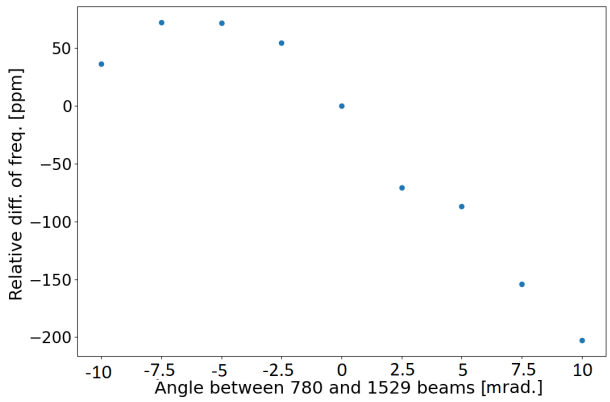

Figure 20: Relative difference of frequency as a function of the angle between the IR and NIR ray in the interferometer, horizontal variation

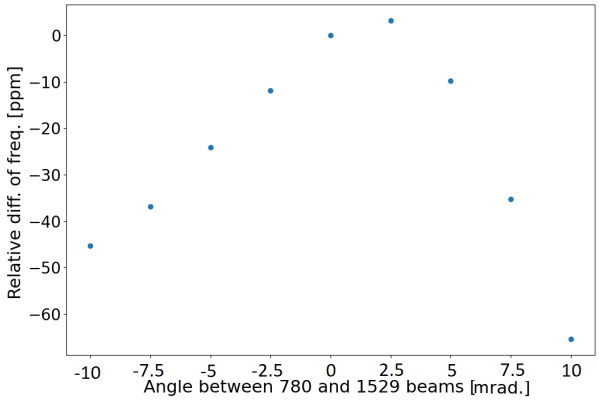

Figure 21: Relative difference of frequency as a function of the angle between the IR and NIR ray in the interferometer, vertical variation

The specification of the piezoelectric translation stage gives us an uncertainty on the Yaw of ± 20 μm, so we tried a modelling in which we have a linear yaw that depends on the position of the translation stage(such as if we define β as the angle of the mirrors, we have $\beta(z) = \beta' z$).

If we take the formula computed in the appendix, which works only for one of the two axes (the vertical one) we get with α the angle between the IR and NIR ray in the interferometer and $\Delta(0)$ the difference in optical path in the interferometer when the translation stage is at it's initial position

$$\frac{\phi_{IR}(z) - \phi_{IR}(0)}{\phi_{NIR}(z) - \phi_{NIR}(0)} = \frac{k_{IR}}{k_{NIR}}(1 - \alpha^2 + \beta' \alpha \Delta(0)) + o(\alpha^2, z = 0)$$

which gives us the quadratic variation of the wavelength with respect to the angle between the two rays (for the other axis the formula is similar but not the same). Moreover, we can write this as

$$\frac{\phi_{IR}(z) - \phi_{IR}(0)}{\phi_{NIR}(z) - \phi_{NIR}(0)} = \frac{k_{IR}}{k_{NIR}}(1 - (\alpha - \frac{\beta' \Delta(0)}{2})^2 + (\frac{\beta' \Delta(0)}{2})^2) + o(\alpha^2, z = 0)$$

With α the angle between the IR and the NIR beams and Δ is $l_{m1} - l_{m2} = \Delta(z)$ with l_{mi} the distance of the mirror i of the interferometer to the beam splitter as explained in the section 7.2 of the annex. This formula explain why we have this linear response locally on 0 of the precision with respect to the angle between the IR and NIR ray in the interferometer which impair the trueness of measurement.

So here in the computation of uncertainties, we have $\frac{\delta \lambda_{IR}}{\lambda_{IR}} = \beta' \alpha \Delta(0) = 3 \times 10^{-5}$ with $\beta' = \frac{40 \times 10^{-6}}{120 \times 10^{-6}} = 0.3$ (The translation stage is L $= 120 \mu m$ and we take $\beta(L) = 40 \mu rad$ as the yaw is $\pm 20 \mu m$), $\alpha = 10^{-3}$ (with an alignment with the eye of the NIR and IR rays at the output of the interferometer at 1 m) rad and $\Delta(0) = 0.1m$.

After several attempt to understand why such error exist in the first place, we finally understood that using plane mirror and not using a corner reflector as in [11] which send back the rays with the same angle whatever the angle of the deck, may impair our measurement.

We can now construct a tab that resume every uncertainties encountered.

Uncertainty source	Relative uncertainty	Parameter uncertainty
Temperature	9.53×10^{-7}	$\delta T = 1K$
Pressure	2.65×10^{-9}	$\delta P = 1kPA$
Humidity	1.92×10^{-8}	$\delta RH = 1\%$
Optical Index	6×10^{-8}	$\delta n = 3.2 \times 10^{-8}$
Gouy Phase	1.2163×10^{-7}	/
Angle IR/NIR	3×10^{-5}	$\delta\alpha = 10^{-3}rad$

5 IR locking

5.1 Set-up

The IR Locking System :

In this section we will explain the general principle used to lock the IR laser, the general idea is explained in [2].

Firstly we take into consideration only the NIR laser, as shown in the Figure 22, it make a single pass through a rubidium cell. It will be the "pump". The next step is to add symmetrically the IR laser, which is finally analysed in a photo-diode, it is the "probe".

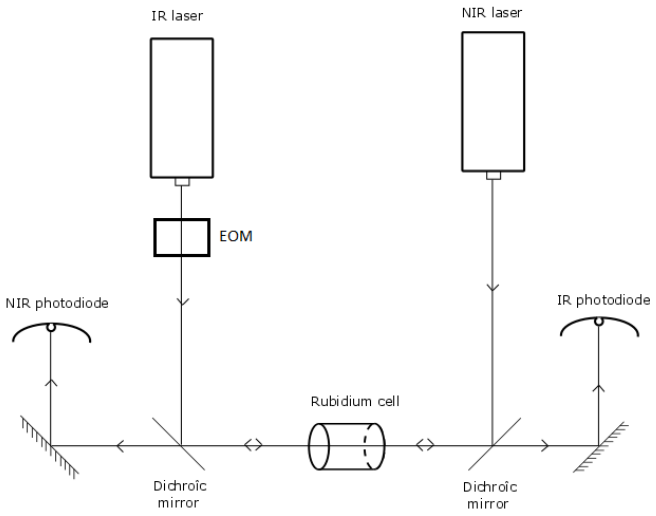

Figure 22: Schematic of the IR locking

The next step in order to lock the laser is to have an approximate idea of the appropriate set of current and temperature (I,T) of the laser in order to have the right wavelength. Otherwise we would have to try at lot of combinations of the two parameters hoping to find the right one.

Given that the NIR laser is locked on the crossover between $(5S_{1/2}, F = 2 \longrightarrow 5P_{3/2}, F^{'} = 1)$ and $(5S_{1/2}, F = 2 \longrightarrow 5P_{3/2}, F^{'} = 3)$, we have the velocity of the class of atoms that are resonant with the laser, we can then deduce the absolute frequency of the locked IR laser knowing that we want to lock it on the transition $(5P_{3/2}, F^{'} = 3 \longrightarrow 4D_{5/2}, F^{"} = 4)$ (see Figure 3). It is a two photon transition, the first transition is saturated by the pump, which is the NIR laser. Because only a given class of atoms is excited to the intermediate state and thus we have a sharp spectral line for the IR. We can compute the laser frequency $f_{laser,IR}$ knowing the atomic transition frequency $f_{at,IR}$:

$$f_{laser,IR} = \frac{f_{at,IR}}{1 + \frac{v}{c}}$$

And thus we get $\lambda_{laser,IR} = 1529.368nm$.

5.2 Locking of the IR laser

In order to lock the IR laser, we had to know with some extent what are the associated current and temperature that would give us the wavelength that is close enough to the atomic resonance we are looking for locking. In this part we show how we used the spectrometer to get the good value of current and temperature of the laser.

Firstly what we want to do is to propose a linear model of the variations of wavelength induced by the two parameters that are the current and the temperature. So we locally map these variations :

We measured λ_{IR} as a function of the current of the IR laser from 60 mA to 72.5 mA with steps of 0.5 mA. Each points is the mean of 320 measurements and the error is (np.std/$\sqrt{N}$) the estimated standard error of the mean.

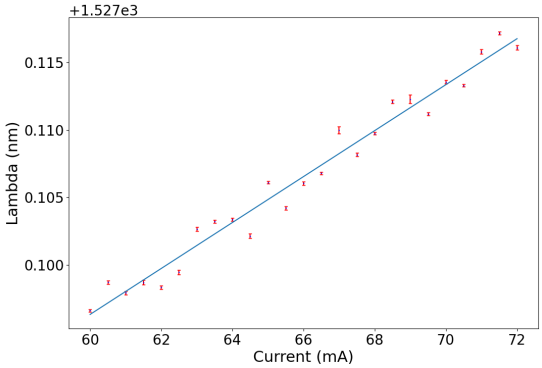

Figure 23: λ_{IR} (nm) function of the current (mA)

Parameters of a linear fit $ax + b$:

$a = 1.7.10^{-3} nm/mA$

$b = 1.52699.10^{3} nm$

We measured λ_{IR} as a function of the temperature of the IR laser from 25.0°C to 29.7°C with steps of 0.1°C. Each points is the mean of 320 measurements and the error is (np.std/$\sqrt{N}$) the estimated standard error of the mean.

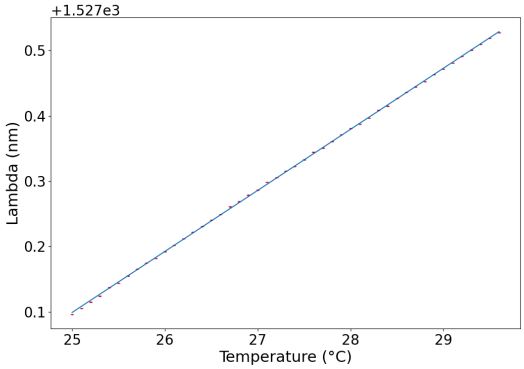

Figure 24: λ_{IR} (nm) function of the temperature (°C)

Parameters of a linear fit $ax + b$:

$a = 9.3.10^{-2} nm/°C$

$b = 1.5269.10^{3} nm$

Out of this linear mapping of the wavelength, we can extrapolate these variations and pick a set of parameters (I, T) out of this linear map that would gives us the wanted wavelength (there is an infinite number of such parameters, we picked one that seem adapted to the laser), we then only modified the current parameter around the value I in order to find the spectral line for the IR laser.

So in order to reach the approximately the desired wavelength, we had to pick the set (381.3mA,33°C) and modify the current in order to find the atomic transition characterized by a spike of transmission on a Doppler gap.

This way we locked the IR laser on the desired transition and thus we precisely know its wavelength, the feedback loop is done with a home-built digital PID circuit based on a RedPitaya STEMlab 125-14 board.

6 Conclusion

During my four month internship in the Quantum Photonics' team of the "Collège de France", I have set-up the lock of an IR laser and a wavemeter which allow the accurate measurement of its wavelength with a precision two-beam scanning Michelson interferometer. These two set-ups are tightly linked with the main experiment of the Quantum Photonics' team which will make use of this laser's lock to induce strong interaction between photons inside the cavity through the strong interactions between atoms in the cold cloud.

The locking of the IR laser is successful and the wavemeter has been characterized (its relative statistical precision of $1.30.10^{-6}$ and its trueness on the wavelength on which we lock the IR laser with a relative precision of $4.31.10^{-5}$). The wavemeter that has been presented here have several interesting point such as the short distance on which the translation has to sweep (120 μm) and the relatively short time for each sweep (50ms) which can compete with an industrial wavemeter which usually sweep on distances of several centimeters in seconds.

This internship has required me to acquire new technical skills such as optical set-up, electronics assembly and data acquisition. As well, I had to learn new knowledge such as hardware description language programming (SystemVerilog), treatment of signals and various physical concept (laser locking, PID, saturated absorption spectroscopy,etc ...). Furthermore I had to consolidate my knowledge in various other domain such as Python programming, atomic physics, laser's physics, restrained relativity, optics and uncertainties in science.

Finally, I had the opportunity to discover the experimental laboratory's environment which has a really important role in the seeking of my future career. The diversity of knowledge required to work in such environment is what struck me the most during my internship. This quantity of "transverse" knowledge is not a problem in itself but make me wonder if the ones involved in experimental physics are the ones I want to learn and use during my everyday work. I'm fairly more interested in the one required in simulation and theoretical physics which will most likely be the matter of my M2's internship. Nevertheless, it was a wonderful experience to work in an experimental laboratory for which I thanks the whole team that have welcomed me for this internship.

7 Annex

7.1 Fourier Transform vs Curve fitting

This subsection address the question of why we can't just apply a discrete Fourier transform in order to extract the wavelength we are looking for and why we have used a curve fitting instead.

First of all, there is a distinction between a Fourier transform and a Fourier series. These mathematical objects are deeply related but have subtle differences such as the set we are considering and the theorems demonstrating their utility (reversibility for the Fourier transform and convergence for the Fourier series).

In our set-up, the translation stage has a finite excursion which is quite small ($100\mu m$), so our signal is restricted in this small compact subset of R. The precision of a Fourier series in such compact is directly linked to the length of this compact, in our case it's so small that the precision is insufficient. The main thing to understand is that when we calculate a Fourier series, we only expand our function on a set of periodic functions sufficiently smooth in the considered set. Given a compact and the form of the function (which are of the form e^{ikx}) which explain the maximum resolution. This legitimate the use of a more complicated way of computing the infrared wavelength

If we want to theorize the question of the efficiency of the process of the data treatment, we have to take into account how we use the acquired data. When one have enough translation length, one can sometime just count the number of local maxima with the initial and the final phase of the signal in order to have a sufficient precision. When looking at the loss of data in this process, it seems to be quite high (just consider for example that we have 8 points per period and we use just a few in order to get the maximums). On the other hand, our program which is based on the fitting of curves, we use use all of the data, which can explains why it's so efficient compared to the one discussed.

However, saying that we use only a little portion of the data when looking only at the extrema is false as we require the other points to pinpoints the fact that they are extrema. Moreover the precision at which we know they actually are extrema highly depends on the other acquired points : if we have for example 3 points per period, the probability that one of these is close enough to the actual extrema is not as high than when we have twice as much points per period, so there is still questions about the difference in efficiency between our process and the others'.

7.2 Computation of the angle study

In this annex we derive the angle (between the IR and the NIR ray in the interferometer) dependence of the absolute precision of the measurement. As explained before there are two possibilities (pitch or yaw).

Firstly let's suppose that locally at the deck, the optical axis is x (so the mirrors are in the (y,z) plane). We can easily understand that the mirrors may undergo effects such as yaw, pitch or roll effect which can impair the measurement precision. Because of the symmetry of our problem, the roll has no importance whatsoever.

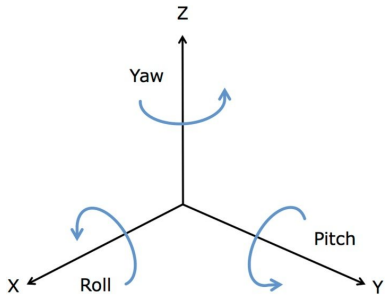

Figure 25: Schematic of the yaw, pitch and roll

These effects can be easily found in the specifications of the translation stage, which will help us to model this effect. We will suppose that in a sweep (a measurement) the angle between the first position and the last is linear from 0 to the maximum of the specification. $\beta(z) = \beta^{'} z$ with A a constant which depend on the maximum specification and the range of the deck. We will only do the computation for the yaw.

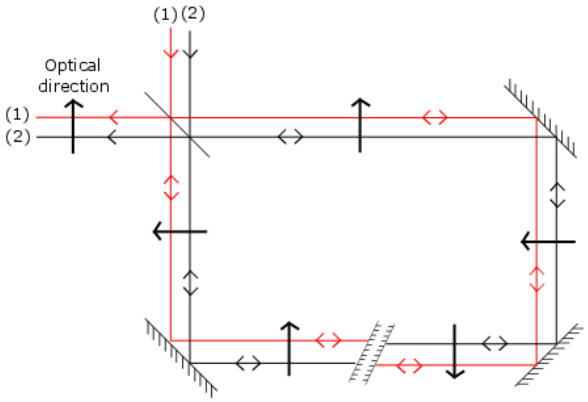

Figure 26: Schematic of the interferometer from top to bottom

In Figure **??** the red and the black rays are from the same laser's beam and emphasize the optical direction which vary at every mirror. The optical direction gives the positives of the perpendicular axis to the optical axis : it enables to understand what angle the beam encounter at the translation stage's mirrors. Assuming that both mirrors of the translation stage have the same angle with respect to z (the position of the translation's stage) then if we unwrap the optical path in order to have both

arms of the interferometer in the same figure, then both rays that bounce back on a mirror have the same angle (and not the opposite in the case of the pitch).

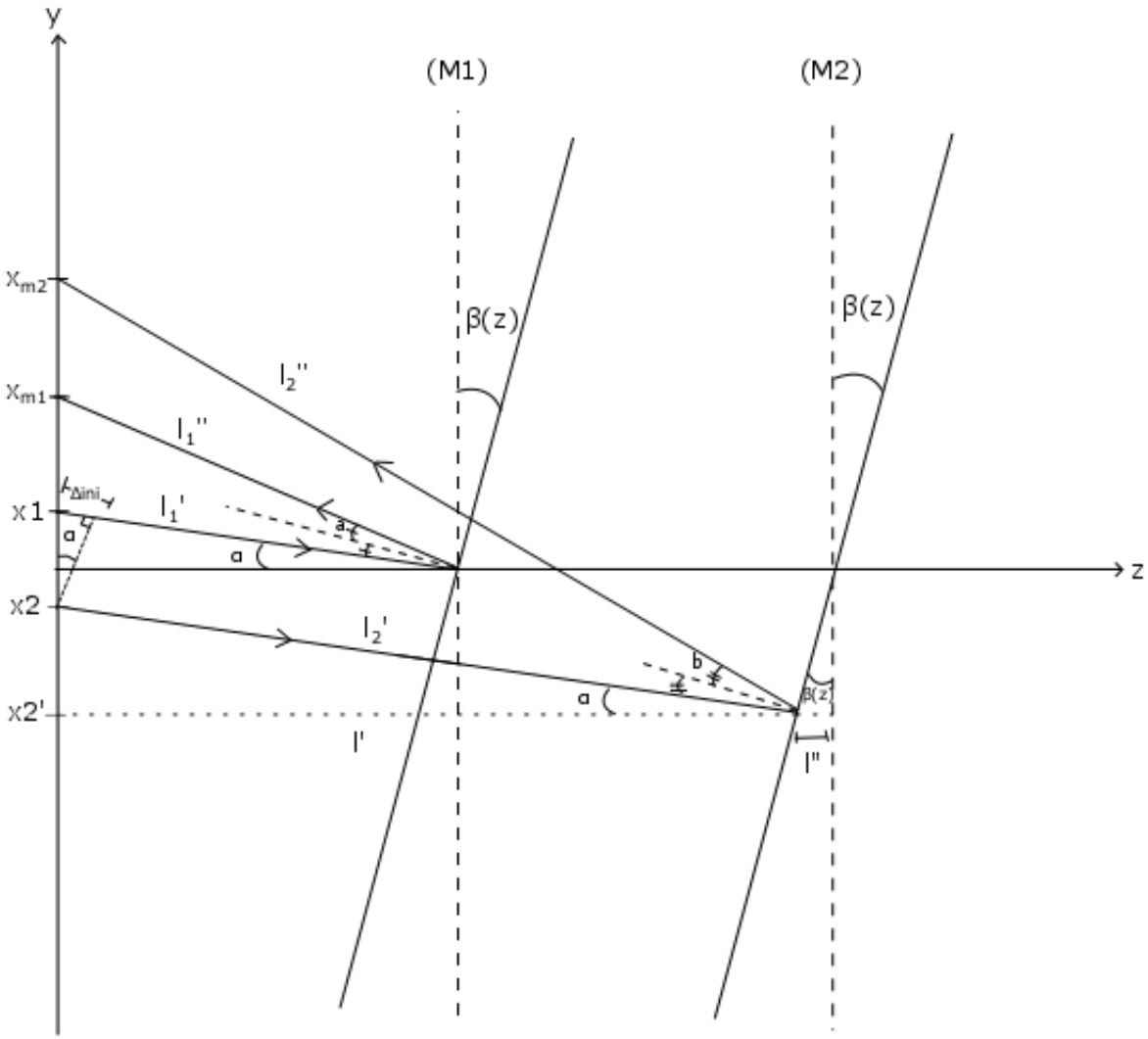

Figure 27: Modelisation of the problem

Here is the schematics of the model if we look from upside down. Let's denote l_{m1} and l_{m2} the (M1)'s and (M2)'s (the two mirrors of the translation stage of the interferometer) position on the z axis. If we unwrap the path of the two rays in the interferometer, we get this schematics. The first ray has a given height x_1 and the second ray a height x_2 initially. Let's denote $l_{opt,i}$ the associated optical path to ray i. We want to compute these two optical path imposing $x_{m1} = x_{m2}$ and have their

value only as function of $\alpha, \beta, l_{m1}, l_{m2}$ and use x_2 and l' as intermediate of calculus.

$$\begin{aligned} \mathrm{l}_{opt,1} &= l_1^{'} + l_1^{"} \\ l_{opt,2} &= l_2^{'} + l_2^{"} - \Delta ini \end{aligned} \tag{9}$$

We subtract Δini our of $l_2^{'} + l_2^{"}$ in order to take into account the correct optical path of the second ray with respect to the first one.

Firstly we compute $l_{opt,1}$: Let's denote $\gamma = 2\beta - \alpha$ (a=b because the two rays arrive with the same angle and bounce on a mirror which have the same angle with the optical axis), we then have $l_{opt,1} = l_{m1}(\frac{1}{cos(\alpha)} + \frac{1}{cos(\gamma)})$. For the second optical path :

$$\begin{aligned} \tan(\alpha) &= \frac{x_2 - x_2^{'}}{l'} \\ l' + l" &= l_{m2} \\ tan(\beta) &= \frac{l"}{-x_2^{'}} \\ l^{'} = l_{m1} - \frac{x_2^{'}}{tan(\gamma)} &\Longleftrightarrow l' = \frac{x_2 - x_2'}{tan(\gamma)} \end{aligned} \tag{10}$$

Out of these equations we get that $l' = l_{m2} + x_2' tan(\beta)$ and we know that $cos(\alpha) = \frac{l'}{l_2'}$, so if we write $l_{m1} = z + l_{m1}(0)$ and $l_{m2} = -z + l_{m2}(0)$, then we can write $l_{m1} - l_{m2} = \Delta(z) = 2z + \Delta(0)$. So out of this we can compute the optical path of the second ray :

$$l_{opt,2} = l'(\frac{1}{cos(\alpha)} + \frac{1}{cos(\gamma)}) - (l_{m1} tan(\alpha) - x_2) sin(\alpha)$$

We can then compute l' and x_2 (we want to know the value of x_2 which allow $x_{m1} = x_{m2}$) :

$$\begin{aligned} \mathrm{l}^{'} &= \frac{l_{m2} + l_{m1} tan(\beta) tan(\gamma)}{1 + tan(\alpha) tan(\gamma)} \\ x_2 &= l^{'}(tan(\alpha) + tan(\gamma)) + l_{m1} tan(\gamma) \end{aligned} \tag{11}$$

We have finally have

$$\begin{aligned} \phi(z) &= k((\frac{1}{cos(\alpha)} + \frac{1}{cos(\gamma)})(l_{m1} - l^{'}) + sin(\alpha)(l_{m1} tan(\alpha) - x_2)) \\ \phi(0) &= k \frac{4(l_{m1} - l_{m2})}{cos(\alpha)} \end{aligned} \tag{12}$$

Now we can expend l' and x_2 at $o(\alpha^2, z)$:

$$\begin{aligned} \mathrm{l}^{'} &\sim l_{m2} + o(\alpha^2, z) \\ x_2 &\sim -\alpha l_{m2} + (l_{m1} + l_{m2}) 2\beta^{'} z + o(\alpha^2, z) \end{aligned} \tag{13}$$

Then we can expend at the same order $\phi(z)$

$$\phi(z) \sim k(2(2z + \Delta(0)) + 2\alpha^2(2z + \Delta(0)) - 4\beta^{'} z \alpha \Delta(0) + (l_{m1} + l_{m2})\alpha^2 + 2\alpha(l_{m1} + l_{m2})\beta^{'} z + o(\alpha^2, z)$$

And thus we can compute

$$\frac{\phi_1(z) - \phi_1(0)}{\phi_2(z) - \phi_2(0)} = \frac{k_1}{k_2}(1 - \alpha^2 + \beta' \alpha \Delta(0)) + o(\alpha^2, 0)$$

References

[1] Nathan Schine Claire Baum Alexandros Georgakopoulos Jonathan Simon Logan W. Clark, Ningyuan Jia. Interacting floquet polaritons. 2019.

[2] Simon Coop Thomas Vanderbruggen Krzysztof T. Kaczmarek Y. Natali Martinez de Escobar, Silvana Palacios Alvarez and Morgan W. Mitchell. Absolute frequency references at 1529 nm and 1560 nm using modulation transfer spectroscopy. 2015.

[3] Doppler broadening. Available at `https://en.wikipedia.org/wiki/Doppler_broadening`.

[4] Daniel A. Steck. Rubidium 87 d line data. 2001.

[5] Long Zhe Li Jong-Dae Park Heung-Ryoul Noh, Sang Eon Park and Chang-Ho Cho. Modulation transfer spectroscopy for 87rb atoms: theory and experiment. 2011.

[6] D. Bloch S. Le Boiteux and M. Ducloy. Theory of optical heterodyne three-level saturation spectroscopy via collinear non-degenerate four-wave mixing in coupled doppler-broadened transitions. 1985.

[7] Daryl W. Preston. Doppler-free saturated absorption: Laser spectroscopy. 1996.

[8] G. C. Bjorklund and C. Ortiz M. D. Levenson, W. Lenth. Frequency modulation (fm) spectroscopy. 1983.

[9] Gary C. Bjorklund. Frequency-modulation spectroscopy: a new method for measuring weak absorptions and dispersions. 1979.

[10] Edward A. Whittaker James M. Supplee and Wilfried Lenth. Theoretical description of frequency modulation and wavelength modulation spectroscopy. 1994.

[11] J. E. Thomas N. A. Kurnit A. Szöke F. Zernike P. H. Lee J.-P.Monchalin, M. J. Kelly and A. Javan. Accurate laser wavelength measurement with a precision two-beam scanning michelson interferometer. 1981.

[12] M Vedel C Champenois Martina Knoop J Pedregosa-Gutierrez, D Guyomarc'h. Computer-controlled high-precision michelson wavemeter. 2014.

[13] Josselin Garnier. *Gestion des incertitudes et analyse de risque*. Ecole polytechnique, 2019.